

Malnutrition delayed wound healing after tooth extraction by HMGB1-related prolonged inflammation

Yao Zhang^a, Hidetaka Ideguchi^a, Hiroaki Aoyagi^a, Keisuke Yamashiro^{b,d}, Tadashi Yamamoto^a, Masahiro Nishibori^c, Shogo Takashiba^{a,*}

^a Department of Pathophysiology - Periodontal Science, Okayama University Graduate School of Medicine, Dentistry and Pharmaceutical Sciences, Okayama, Japan

^b Department of Periodontics and Endodontics, Okayama University Hospital, Okayama, Japan

^c Department of Pharmacology, Okayama University Graduate School of Medicine, Dentistry and Pharmaceutical Sciences, Okayama, Japan

^d Present address: Department of Oral Health, Kobe Tokiwa University, Hyogo, Japan

ARTICLE INFO

Keywords:

Malnutrition
Tooth extracted wound
Inflammation
HMGB1
IL-1 β
Wound healing

ABSTRACT

Malnutrition causes prolonged inflammation, resulting in delayed wound healing. High mobility group box-1 (HMGB1) is a damage-associated molecular pattern that is present in the nuclei of macrophages and is secreted into the extracellular milieu in response to stimuli. It stimulates the production of interleukin-1 β (IL-1 β) through the receptors for advanced glycation end products (RAGE), inducing an inflammatory response, which is an essential response to initiate wound healing. We hypothesized that malnutrition may interfere with this cascade, causing abnormal inflammation and ultimately delaying wound healing. We used tooth-extracted mice with malnutrition fed with low-casein diet for two weeks. On days 3 and 7 after tooth extraction, the wound tissue was histologically observed and analyzed for several factors in the inflammation-regeneration lineage, including IL-1 β , mesenchymal stem cells, myeloperoxidase activity, HMGB1, macrophage polarization, and adenosine 5-triphosphate (ATP). On day 7, delayed wound healing was observed with the following findings under malnutrition conditions: decreased mRNA expression of genes for regeneration and mesenchymal stem cell (MSC) accumulation, an obvious increase in myeloperoxidase and IL-1 β mRNA expression, an increase in HMGB1 levels, and an increase in ATP concentration in tissues with elevated proportion of M2 macrophages. These results suggest that the significantly increased secretion of HMGB1 associated with the upregulated production of ATP and IL-1 β secretion via the RAGE pathway may interfere with the resolution of inflammation and wound healing under the state of malnutrition.

1. Introduction

Through rapid global nutrition transition, an increasing proportion of individuals are exposed to malnutrition during their life course. Malnutrition is a frequent and serious condition of multifactorial origin and is associated with adverse consequences. Elderly people in developed countries and children aged below 5 years in low-income and middle-income countries experience this condition [1–3]. Malnutrition is not only affected by rapidly changing diets, norms of eating, and physical activity patterns, but also by pathogen burden and extrinsic mortality risk [4]. It is generally believed that insufficient protein intake accompanied by malnutrition damages the innate or acquired immune function by imposing a high metabolic load on a depleted capacity for

homeostasis [5]. It increases the risk of developing non-communicable diseases and long-term chronic inflammation, such as cardiovascular disease, atherosclerosis syndrome, and chronic kidney disease [5–9]. Malnutrition is strongly associated with oral diseases. Poor oral health may affect food selection and nutritional intake, leading to malnutrition [10]. Similarly, malnutrition affects the development and integrity of the oral cavity, the progression of oral diseases, and the physical and chemical properties of saliva [11]. Consequently, a vicious circle is established. Malnutrition impairs wound healing and increases the risk of secondary infections [12].

Wound healing has four processes: coagulation, inflammation, migration and proliferation, and remodeling. Inflammation usually occurs due to the localization and elimination of damaged factors and

* Corresponding author at: Department of Pathophysiology - Periodontal Science, Graduate School of Medicine, Dentistry and Pharmaceutical Sciences, Okayama University, 2-5-1 Shikata-cho, Kita-ku, Okayama 700-8525, Japan.

E-mail address: stakashi@okayama-u.ac.jp (S. Takashiba).

<https://doi.org/10.1016/j.intimp.2021.107772>

Received 23 March 2021; Received in revised form 5 May 2021; Accepted 5 May 2021

Available online 24 May 2021

1567-5769/© 2021 The Author(s). Published by Elsevier B.V. This is an open access article under the CC BY license (<http://creativecommons.org/licenses/by/4.0/>).

promotes the healing of damaged tissues [13]. However, the recruitment of cells and mediators is changed during impaired wound healing. It prevents cell proliferation and injury healing and leads to continuous chronic inflammation. It has been shown that biomimetic and biocompatible wound dressings, such as hyaluronic acid, are beneficial to wound healing [14–16]. However, it remains unclear whether delayed healing of the extraction wound under malnutrition conditions is related to prolonged inflammation. Despite the proven consequences of malnutrition, the lack of research on its mechanisms still limits its treatment. Traditional treatment methods usually use improved and complementary interventions, such as physical activity training and oral nutritional supplements [17]. However, these long-term processes have little effect on wound healing, as the level of malnutrition cannot be improved immediately. Therefore, the mechanism of long-term chronic inflammation should be emphasized when developing new treatment methods for malnutrition.

High mobility group box-1 (HMGB1) belongs to the high-mobility group nuclear protein family. It is a DNA-binding protein mainly present in monocytes, especially macrophages, and functions both inside and outside the cell. HMGB1 is involved in proper transcriptional regulation, DNA recombination, and maintenance when located in the nucleus. It is released when there is danger-induced cellular stress, which regulates inflammation and regeneration of extracellular signaling molecules as one of damage-associated molecular pattern molecules (DAMPs) [18]. Toll-like receptors (TLRs) and receptors for advanced glycation end products (RAGE) are the main HMGB1 receptors. Excessive production of extracellular HMGB1 may cause tissue damage and organ dysfunction in individuals with infertility and infectious diseases. HMGB1 easily binds to other pro-inflammatory molecules, including DNA, RNA, histones, nucleosomes, lipopolysaccharide (LPS), stromal cell-derived factor 1/chemokine receptor type (CXCR4), interleukin-1 (IL-1) α , IL-1 β , and other factors that trigger inflammation. In addition, HMGB1 acts as a pro-inflammatory mediator. Extracellular HMGB1 is transformed into an effective activator of pro-inflammatory cytokine production through RAGE and TLR receptor stimulation [19]. Bone healing is promoted by inflammation induced by HMGB1 [20], and periodontal inflammation and bone resorption were reduced in mice after the administration of anti-HMGB1 neutralizing antibody [21] based on previous studies conducted in our laboratory.

Long-term chronic inflammation, usually accompanied by malnutrition, may be the cause of delayed healing of tooth extraction wounds. Moreover, HMGB1 has been shown to act on non-infectious inflammation in previous studies. Therefore, we hypothesize that the delayed healing of tooth extraction wounds caused by malnutrition is related to inflammation induced by HMGB1. In this study, we established a malnourished tooth-extracted mouse model to determine the inflammation levels and inflammation-related factors, including HMGB1, ATP, and IL-1 β , at 3 and 7 days after tooth extraction. In addition, the percentages of two types of macrophages, M1 macrophages and M2 macrophages, were investigated to further elucidate the relevant HMGB1 inflammatory pathways. These results unveiled how malnutrition affects healing of tooth extraction wounds from an inflammatory viewpoint.

2. Materials and methods

2.1. Animal and malnourished Tooth-Extracted mouse model

This study was approved by the Animal Care and Use Committee, Okayama University (Permit no: OKU-2018498 and OKU-2018679). All animal experiments were carried out in accordance with the Guidelines for Animal Experiments of Okayama University.

Ten-week-old male C57BL/6J mice (CLEA, Tokyo, Japan) maintained in individually ventilated cages under a constant temperature of 25 °C with a 12:12 light–dark cycle was used in the experiments. The mice were provided free access to sterile food and water under specific pathogen-free conditions. They were randomized to malnourished

group (N = 4/group), which were fed with 3% casein diet (CLEA), and control group (N = 4/group), which were fed a 25% casein diet (CLEA) [22]. This basic set of mice (total 8 mice/set) was used for following all of experiments (18 sets for whole study). However, in some experiments, 2 sets of mice were used when specified in the figure legend. The mice were initially anesthetized with pentobarbital (50 mg/kg body weight); the left first maxillary molar was extracted as the test site, while the right maxillary molar was left intact as the control site. The mandible and gingival tissues were collected 3 and 7 days after the tooth extraction. The mice were weighed twice a week.

2.2. Hematoxylin-Eosin staining

The mandibular samples containing the extracted socket were dissected, fixed in 4% paraformaldehyde (Wako Pure Chemical, Hiroshima, Japan), decalcified in 10% ethylenediaminetetraacetic acid (EDTA) disodium salt dehydrate (Sigma-Aldrich, St. Louis, MO, USA) for 7 days at room temperature, and then embedded in paraffin wax. Next, 4- μ m thick coronal serial sections were mounted in serial order on poly L-lysine-coated slides (Matsunami Glass, Osaka, Japan), stained with Mayer's hematoxylin solution and Eosin Y (Merck KGaA, Darmstadt, Germany), and observed under a light microscope using ImageJ software (NIH, Bethesda, MD, USA).

2.3. Quantitative reverse Transcription-Polymerase chain reaction

Total RNA was collected from the maxillary gingival tissue using the RNeasy Plus kit (Qiagen, Hilden, Germany), and the reverse transcription reaction was carried out from 1 μ g of total mRNA using 10 μ M deoxynucleotide triphosphate (dNTP) mix, 50 μ M oligo (dT)12–18 Primer, 5 \times first standard buffer, 0.1 M dithiothreitol, and SuperScript III Reverse Transcriptase according to the manufacturer's protocols (all were purchased from Thermo Fisher Scientific, Waltham, MA, USA).

The primers were designed as follows using the Primer3 online software (<http://frodo.wi.mit.edu/>): for glyceraldehyde-3-phosphate dehydrogenase (GAPDH), 5'-GAGTCAACGGATTTGGTCGT-3' and 5'-GACAAGCTTCCCGTTCTCAG-3'; for CD44, 5'-GCTCCCTCCCTTTAGGTCA-3' and 5'-AAAAGTTGTCATGGCGTGC-3'; for Nanog, 5'-CGG TGGCAGAAAAACAGTG-3' and 5'-AAGGCTTCCAG-ATGCGTTCA-3'; for runt-related transcription factor 2 (Runx2), 5'-GCACTGGGTCA-CACGTATGA-3' and 5'-CCCAC-TGTGAATCTGGCCAT-3'; for IL-1 β , 5'-GTGCTCAGGGTCACAAGAA-3' and 5'-CCACAGTTGACAGCTAGGT-3'; and for CCL2, 5'-AGCCAAGTCTACTGAAGCC-3' and 5'-GCGTTAA CTGCATCTGGCTG-3' (All were synthesized by Eurofins Scientific, Luxembourg). Quantitative reverse transcription-polymerase chain reaction (qRT-PCR) was performed using an ABI 7300 system (Applied Biosystems, CA, USA) at 95 °C for 10 min, followed by 40 cycles at 95 °C for 15 s and 60 °C for 1 min in 96-well plates in a final volume of 20 μ L containing SYBR Green PCR Master Mix (Thermo Fisher Scientific). The relative quantities of transcripts were calculated following the comparative threshold cycle ($\Delta\Delta$ CT) method [23] using GAPDH as the endogenous control. The relative mRNA expression ratio was calculated at each time point as the ratio of the malnutrition group/normal food group.

2.4. Flow Cytometry

Gingival tissue was added to Minimum Essential Medium-alpha with L-glutamine and phenol red (Wako Pure Chemical), 10% deactivated fetal bovine serum (Biological Industries, Kibbutz Beit-Haemek, Israel), 3.2 mg/mL collagenase type IV (Gibco Cell Culture, Carlsbad, CA, USA), and 1 mg/mL deoxyribonuclease I (Sigma-Aldrich), and homogenized using a tissue homogenizer (Ina Optica, Osaka, Japan). The gingival tissue was detached using 0.5 M trypsin EDTA (Gibco) after shaking at 37 °C for 55 min. The cells in the supernatant were recovered by brief centrifugation for analysis. Cell viability was analyzed by staining with

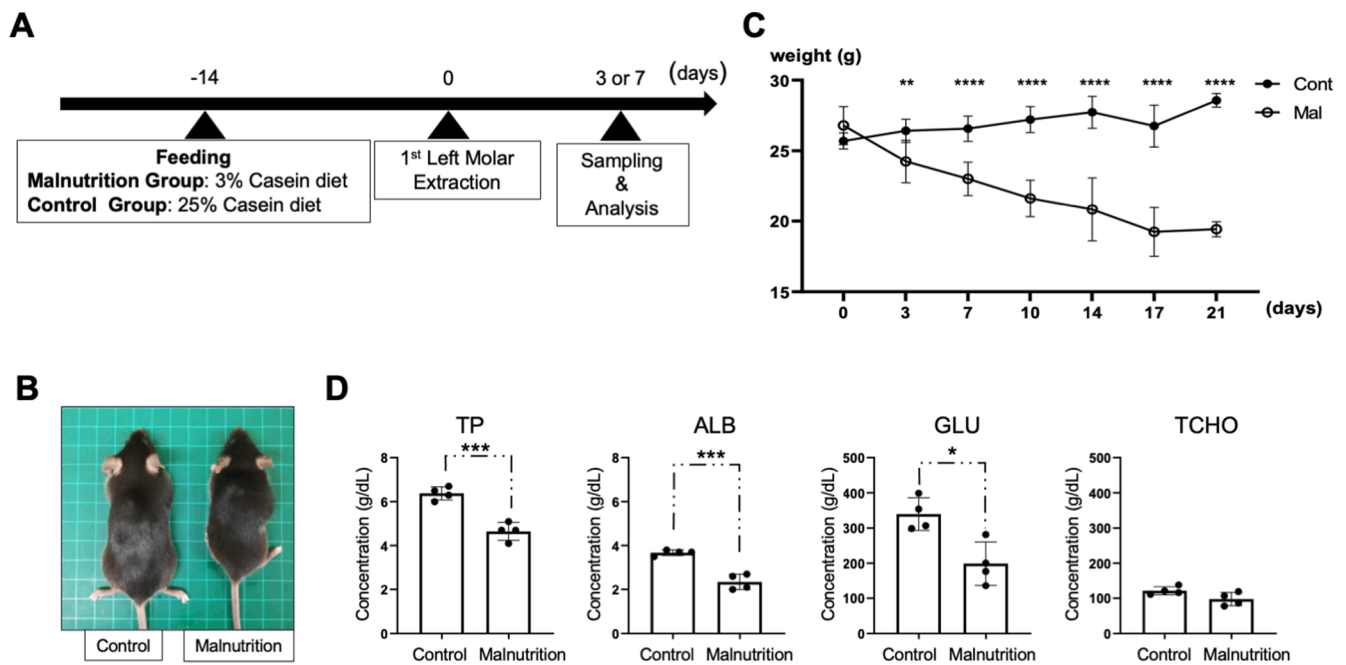


Fig. 1. Experimental protocol and establishment of malnourished mouse model. **A:** The malnourished and control groups were fed with 3% casein diet and 25% casein diet for 2 weeks, respectively; then, the left first maxillary molar was extracted. After 3 and 7 days, the samples were harvested. Malnutrition was confirmed through weight measurements and blood tests. **B:** Malnourished mice were smaller than healthy mice. One of the typical results from panel C. **C:** The mice in the malnourished group continued to lose weight over time compared with the normal mice. Two sets of mice used for blood test and histological analysis with HE staining were measured. **D:** The serum on the day of tissue sample collection was analyzed from 1 set of mice. The concentrations of total protein, albumin, and glucose in the malnourished group were lower than those in the control group. The total cholesterol concentration was not significantly different between the two groups. TP, total protein; ALB, albumin; GLU, glucose; TCHO, total cholesterol. Data are presented as mean \pm SD. Statistical significance is indicated by * $P < 0.05$, ** $P < 0.01$, *** $P < 0.001$, **** $P < 0.0001$. Two-way ANOVA followed by post hoc Bonferroni tests (C) or Student's *t*-test (D) was performed.

the Zombie Violet Fixable Viability Kit (BioLegend, San Diego, CA, USA) and Fc blocking by CD16/32 (BioLegend).

The following dye-conjugated antibodies were obtained from BioLegend: CD44-PE for stem cells, CD140 α -APC/Cy5.5 for mesenchymal-derived cells, CD45-FITC for lymphocytes, CD14b-PE/Cy7 for monocytes, F4/80-Per/Cy5.5 for M ϕ , CD80-APC for M1 M ϕ , CD206-PE/Cy7 for M2 M ϕ , and CD31-APC for platelet/endothelial cells. MSCs were defined as CD44⁺ CD140 α ⁺ CD14b⁻ CD31⁻ CD45⁻, M ϕ was defined as CD45⁺ F4/80⁺, M1 M ϕ was defined as CD45⁺ F4/80⁺ CD80⁺ CD206⁻, and M2 M ϕ was defined as CD45⁺ F4/80⁺ CD80⁻ CD206⁺ using multicolor Flow Cytometry (FCM) utilizing MACSQuant X (Miltenyi Biotec, Bergisch Gladbach, Germany). Data analysis was performed using the FlowJo software (Becton Dickinson Bioscience, Ashland, OR, USA).

2.5. *In vivo* Molecular imaging analysis system

The mice were injected intraperitoneally with 200 mg/kg XenoLight RediJect inflammation probe (PerkinElmer, Waltham, MA, USA). After placing the mice in the IMPAC6 anesthesia chamber attached to the In Vivo Molecular Imaging Analysis System (IVIS) Spectrum (PerkinElmer), the mice were sacrificed 10 min after probe injection. The mandibles were extracted and transferred to the IVIS spectrum, and images were captured after a 5-min exposure for *in vivo* bioluminescence generated by the activity of myeloperoxidase (MPO) as a marker for infiltration of neutrophils. The MPO signals were quantified using Living Image Software V4.4 (PerkinElmer) according to the manufacturer's instructions. In addition, a circular region of interest (ROI) was defined as a region that exhibited more than 50% of the maximum luminescence in the inflammatory site of each mouse. The total flux (measured in photons per second) and maximum radiance (measured in photons per second per square centimeter per steradian) in the ROI were quantified [24].

2.6. Enzyme-Linked Immunosorbent Assay

The connective tissue in the tooth extraction socket was harvested 3 and 7 days after tooth extraction. The concentration of total and released HMGB1 protein in the supernatant of the gingiva was measured using HMGB1 Enzyme-Linked Immunosorbent Assay (ELISA) kit II (Shino-Test, Tokyo, Japan). The absorbance at 490 nm was measured using a microplate reader (Gemini XPS; Molecular Devices, Sunnyvale, CA, USA).

2.7. Immunofluorescence Assay

Paraffin-embedded mandibular sections were prepared as previously described. Immunofluorescence staining was performed according to the standard procedures [19]. For antigen unmasking, the slides were boiled in 1 mM EDTA/PBS (pH 8.0) for 3 min using a microwave. Immunofluorescence staining was performed using a primary antibody against HMGB1 (rabbit polyclonal IgG, 1:100, Shino-Test). The secondary antibody used was Alexa Fluor 488 goat anti-rabbit IgG (1:100, Thermo Fisher Scientific). VECTASHIELD mounting medium with 4,6-diamidino-2-phenylindole (DAPI; Vector Laboratories, Burlingame, CA, USA) was used to prevent rapid loss of fluorescence during microscopic examination and nuclear staining. The measurement area was defined as the same area between each sample from the bottom of the tooth extraction socket.

2.8. Adenosine 5-Triphosphate-Dependent Glycerol-3-Phosphate generation Assay

Fluorometric adenosine 5-triphosphate (ATP) assays were carried out using an ATP Assay Kit (cat. # ab83355, Abcam, Cambridge, UK), following the manufacturer's protocol [25]. Briefly, the gingival tissue was homogenized using a Deproteinizing Sample Preparation Kit (cat. #

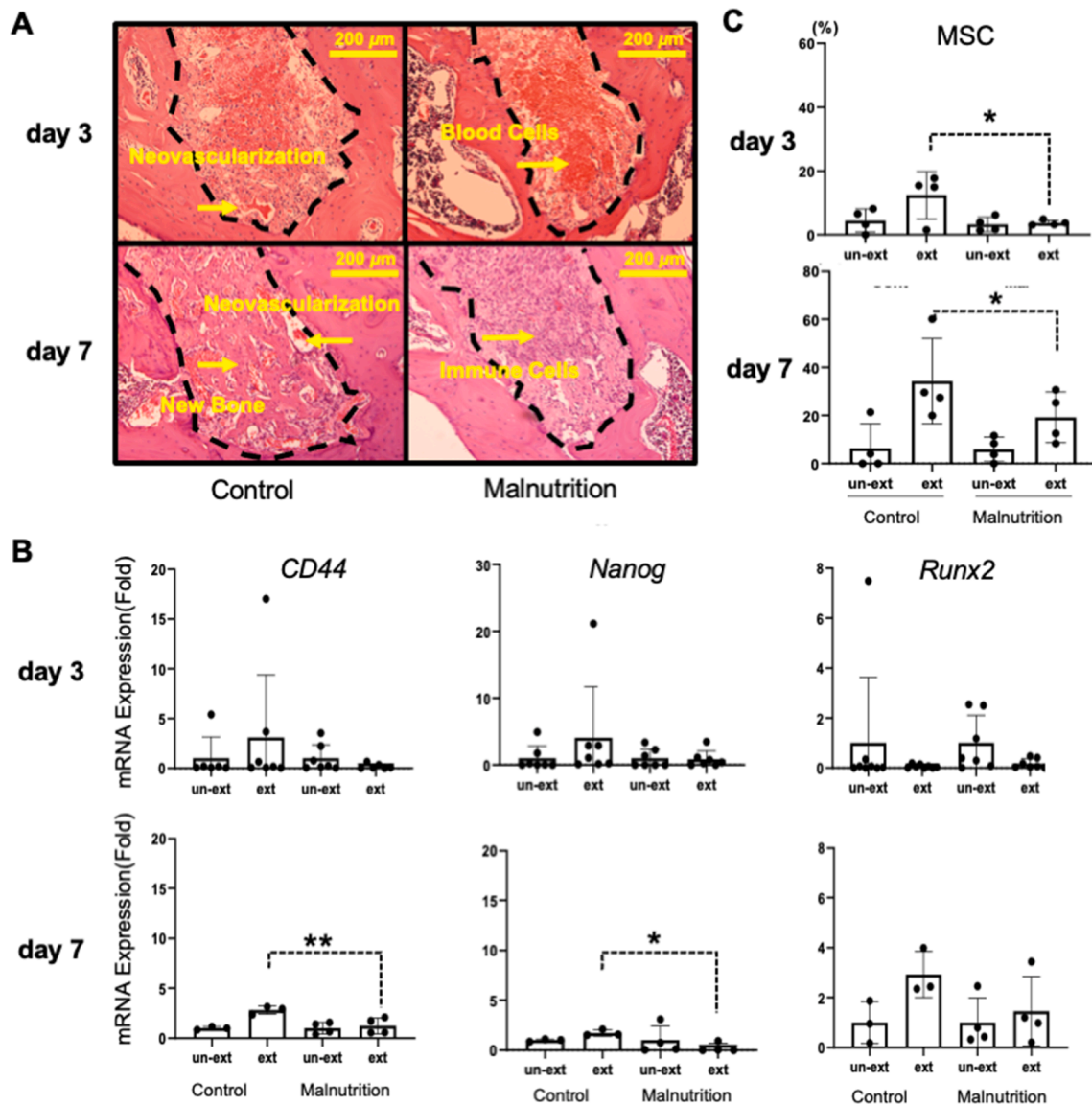


Fig. 2. Hematoxylin-eosin staining of tooth-extracted socket, mRNA expression of regeneration-related genes, and proportion of MSCs in it. **A:** Histological analysis of wound healing in tooth-extracted sockets (HE). On day 3, blood cells were detected in the tooth-extracted sockets of malnourished mice and neovascularization in control mice. On day 7, immune cells were present in the tooth-extracted socket, whereas neovascularization and new bone area were found in the sockets of control mice. One set of mice was used for each day, and a typical section for each condition was shown. **B:** The mRNA expression of *CD44*, *Nanog*, and *Runx2* after tooth extraction was analyzed by quantitative RT-PCR. On day 3, no significance difference was observed; on day 7, the mRNA expression of *CD44* and *Nanog* was not induced in the tooth-extracted socket in malnourished mice compared with that in control mice. Two sets of mice were used for day 3, and 1 set of mice was used for day 7 because of technical issues. **C:** Recruitment of MSCs ($CD44^+ CD140a^+ CD14b^- CD31^- CD45^-$) after tooth extraction was analyzed by FCM and shown as the proportion of MSCs in total cells. The proportion of MSCs was not induced in the tooth-extracted socket in malnourished mice as that in control mice on days 3 and 7. One set of mice was used for each day. un-ext: un-extracted; ext: extracted. Histological images were representative of four independent animal experiments. Scale bar: 200 μ m. Graph data are expressed as mean \pm SD. Results of mRNA expression were normalized to those of *GAPDH* mRNA and were presented as fold change after normalization to the un-extracted group. Statistical significance is indicated by * $P < 0.05$ and ** $P < 0.01$. One-way ANOVA followed by post hoc Fisher's LSD test was performed.

ab204708, Abcam). Samples and standard solutions (50 μ L) were added to the 96-well plates containing the ATP reaction mix and incubated at room temperature in the dark for 30 min. The plates were read using a microplate reader (Gemini XPS; Molecular Devices, Sunnyvale, CA, USA) at Ex/Em = 535/587 nm, and the ATP amount was normalized to the non-extraction side.

2.9. Statistical analysis

For multiple comparisons, statistical significance was evaluated using one-way analysis of variance (ANOVA) followed by post hoc

Fisher's least significant difference (LSD) test, or two-way ANOVA followed by post hoc Bonferroni tests. Student's *t*-test was performed to compare the two groups. A probability value of <0.05 was considered significant. The results were expressed as mean \pm standard deviation. Graphs were generated using GraphPad Prism 8 (GraphPad Software, La Jolla, CA, USA). Schematic representation was produced using Servier Medical Art (<https://smart.servier.com>).

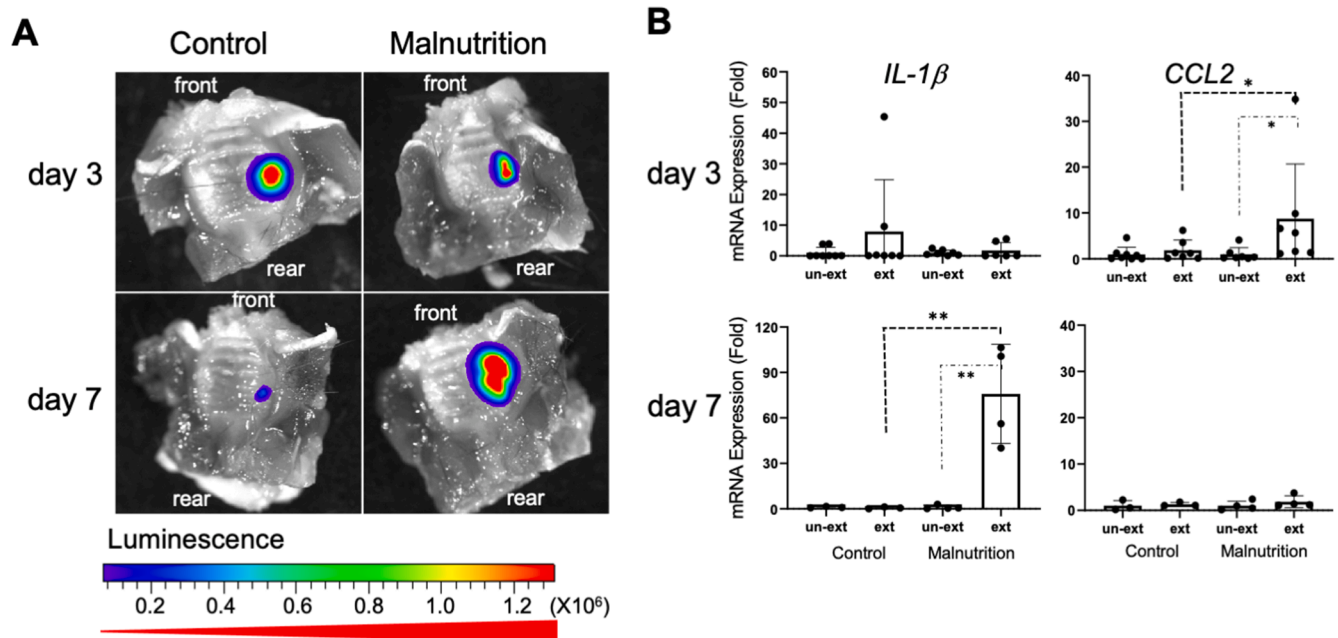


Fig. 3. MPO activity and mRNA expression of pro-inflammatory cytokines in tooth-extracted socket. **A:** Molecular imaging analysis of MPO activity in tooth-extracted sockets. The maxillae were removed on days 3 and 7 after extraction of the left first upper molar. The signal intensity in relation to the total flux and maximum radiance is shown. The typical result was shown from 1 set of mice at each day. **B:** The mRNA expression levels of *IL-1β* and *CCL2* after tooth extraction were analyzed by quantitative RT-PCR. The mRNA expression of *CCL2* increased in the tooth-extracted socket in malnourished mice on day 3 and then decreased to the level of control group, whereas the mRNA expression of *IL-1β* was obviously induced in the tooth-extracted socket in malnourished mice on day 7. Two sets of mice were used for day 3, and 1 set of mice was used for day 7 because of technical issues as shown in Fig. 2B. Graph data are expressed as mean ± SD. Results of mRNA expression were normalized to those of *GAPDH* mRNA and were presented as fold change after normalization to the un-extracted group. Statistical significance is indicated by * $P < 0.05$ and ** $P < 0.001$. One-way analysis of variance followed by post hoc Fisher's LSD test was performed.

3. Results

3.1. Validation of mouse model

A mouse model established by feeding the animal with 3% casein for 2 weeks (Fig. 1A) resulted in a reduction in body weight (Fig. 1B and 1C) and in total protein, albumin, and glucose levels, but not total cholesterol in serum (Fig. 1D).

3.2. Wound healing after tooth extraction

As shown in the hematoxylin-eosin stained image in Fig. 2A, blood cells were still packed in the extraction socket in the malnourished group on day 3 after tooth extraction, although neovascularization was still performed in the control group. In addition, mononuclear cells, probably immune cells, filled the tooth extraction socket in the malnourished group on day 7, whereas new bone was detected in the control group.

When the mRNA expression of genes in mesenchymal stem cells (MSCs) and osteoblasts was detected by qRT-PCR (Fig. 2B), *CD44* and *Nanog* mRNAs tended to be expressed in tooth-extracted socket wounds in the control group on day 3. Although this tendency was upregulated on day 7, it was almost stable or reduced in the wounds of the malnourished group. By contrast, *Runx2* mRNA expression was reduced on day 3 and upregulated on day 7 in both groups. However, no significant difference was observed between the control group and malnourished group. In addition, the population of MSCs increased in the tooth-extracted socket wound and was lower in the malnourished group on days 3 and 7 (Fig. 2C).

3.3. Inflammation after tooth extraction

Although the MPO activity analyzed by IVIS was strong on day 3 in the control group, it almost disappeared on day 7, it was less than that in

the control group on day 3, and it increased on day 7 in the malnourished group (Fig. 3A). The activity on day 7 in the malnourished group was stronger than that on day 3 in the control group.

The mRNA expression of the pro-inflammatory cytokine *IL-1β* tended to increase on day 3 in tooth-extracted socket wounds in the control group, but returned to baseline on day 7. However, it obviously increased in the tooth-extracted socket wound in the malnourished group on day 7 (Fig. 2B: more than 75-folds of un-extracted control in the malnourished group). By contrast, the mRNA expression of a chemokine for monocytes, *CCL2*, obviously increased in tooth-extracted socket wounds in the malnourished group on day 3, but was almost restored to baseline on day 7 (Fig. 2B: more than 8-folds of un-extracted control in the malnourished group). However, this increment was not significant in the tooth-extracted socket wounds in the control group.

3.4. HMGB1 secretion after tooth extraction

HMGB1 in tooth-extracted wound tissue was detected by distinguishing the differences between HMGB1 with intracellular origin and those with extracellular origin (Fig. 4A). After setting the baseline on tooth-un-extracted tissue, the total HMGB1 (intracellular plus extracellular origin) in both control and malnourished groups increased 1.5- to 2.0-folds from day 3 to day 7. In particular, the extracellular HMGB1 increased 1.5-folds in the control group on day 3, but not in the malnourished group. This increment recovered to baseline in the control group on day 7, whereas it remained increase to 1.5-folds in the malnourished group. This resulted in a higher extracellular HMGB1 concentration in tooth-extracted wounds in the malnourished group than in the control group.

The secretion of HMGB1 from the nuclei to the extracellular spaces was detected by conducting an immunohistochemical analysis of the tooth-extracted wound tissue (Fig. 4B). HMGB1 was stained around the nuclei (intracellular space) and extracellular space on day 3 in both the

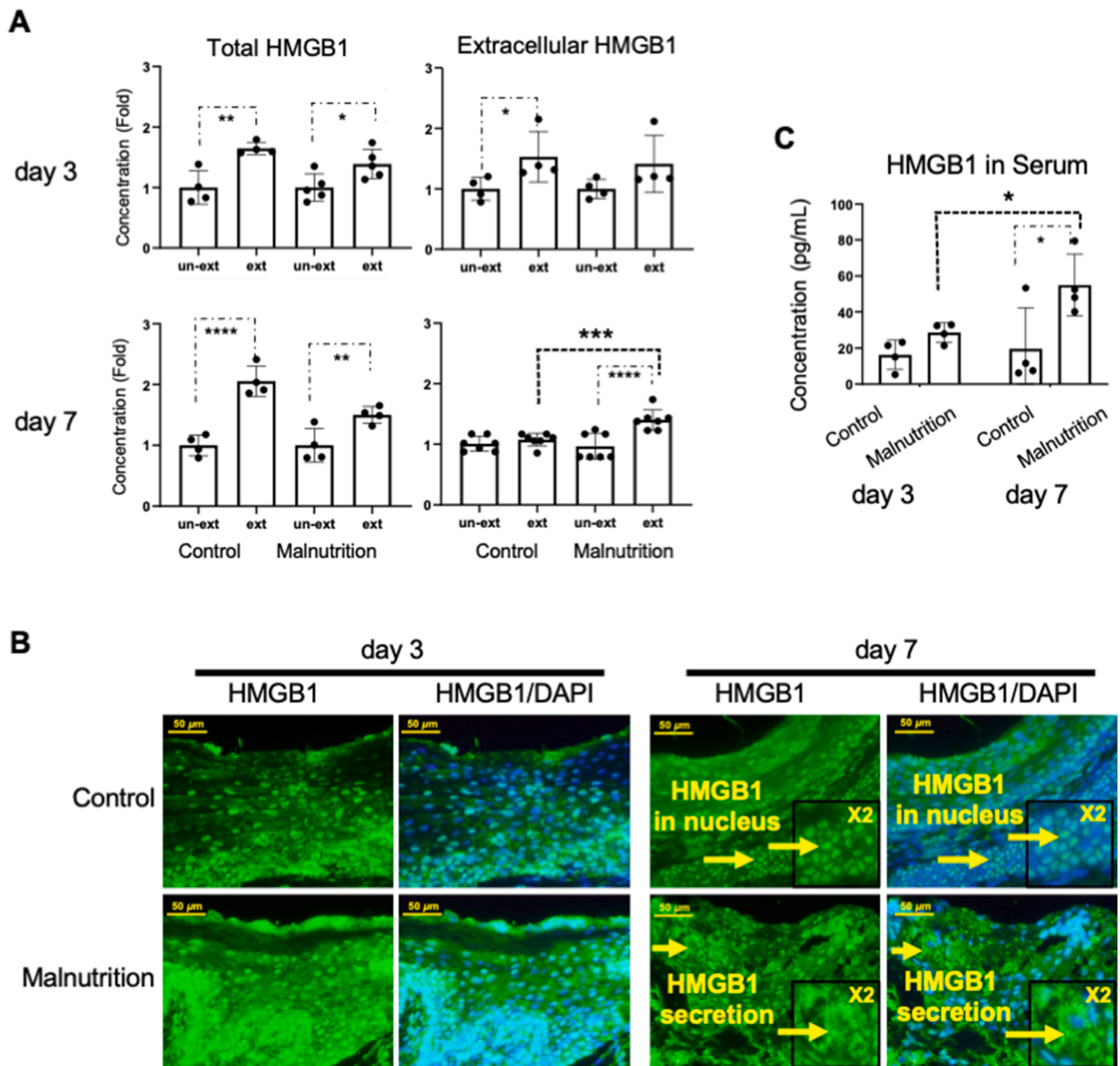


Fig. 4. Localization of HMGB1 in tooth-extracted socket and presence in serum. **A:** Gingival tissue, including a tooth-extracted socket, was homogenized for isolating cellular debris and the aqueous phase. The concentration of HMGB1 in these two groups was analyzed using ELISA. On day 7, extracellular HMGB1 concentration was significantly increased in the tooth-extracted tissue of malnourished mice, although total HMGB1 concentration in tooth-extracted tissue increased of both control and malnourished mice. One set or 2 sets of mice were used for each condition. **B:** In immunofluorescence images of HMGB1 in tooth-extracted sockets in malnourished mice, HMGB1 (green fluorescence) separated from the cell into the extracellular space was detected, especially on day 7. This was clearly observed when the image was superimposed on the image stained for nuclei with DAPI (blue fluorescence). Magnification of the boxed area is shown in the lower-right corner. Yellow arrows indicate HMGB1 staining. One set of mice was used for each day as used in Fig. 2A, and a typical section for each condition was shown. **C:** The concentration of HMGB1 in the peripheral blood was also analyzed using ELISA. Similarly, it increased on day 7. One set of mice was used for each day. un-ext: un-extracted; ext: extracted. Graph data are presented as mean \pm SD. Results are presented as fold change after normalization to the un-extracted group. Statistical significance is indicated by * $P < 0.05$, ** $P < 0.01$, *** $P < 0.001$, and **** $P < 0.0001$. One-way ANOVA followed by post hoc Fisher's LSD test (A) or two-way ANOVA followed by post hoc Bonferroni tests (B) was performed. Scale bar: 50.0 μ m. X2: 2-time magnification.

control and malnourished groups. On day 7, HMGB1 was stained mainly in and around the nuclei in the control group, whereas it was obviously stained in the extracellular space in the malnourished group.

Furthermore, the concentration of HMGB1 in serum also tended to increase in the malnourished group (Fig. 4C). Its concentration significantly increased from day 3 to day 7 in the malnourished group (approximately 2-folds).

3.5. M1/M2 Macrophage polarization after tooth extraction

FCM analysis of the M ϕ proportion revealed that there were no differences among the groups for M1 M ϕ and M2 M ϕ on day 3. On day 7, no differences were observed between the tooth un-extracted and extracted tissues for M1 M ϕ and M2 M ϕ in the control group. On day 7, M1 M ϕ was obviously decreased, whereas M2 M ϕ was obviously increased (Fig. 5).

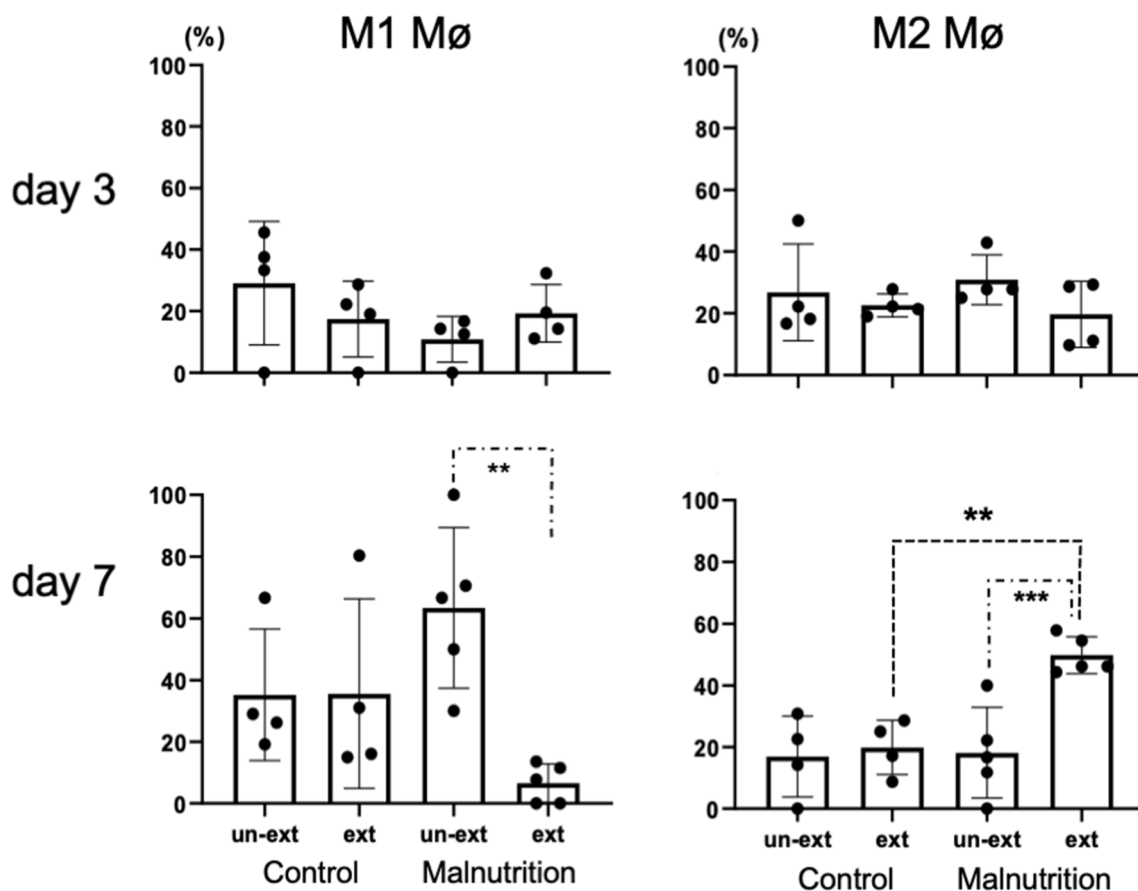


Fig. 5. M1/M2 macrophages ($M\phi$) polarization after tooth extraction analyzed by FCM. The proportion of M1 $M\phi$ ($CD45^+ F4/80^+$, $CD80^+$, $CD206^-$, or M2 $M\phi$ ($CD45^+ F4/80^+$, $CD80^-$, and $CD206^+$) in total $M\phi$ ($CD45^+ F4/80^+$) is shown. No statistical difference was observed between M1 $M\phi$ and M2 $M\phi$ in malnourished and control mice on day 3. However, M2 $M\phi$ increased significantly in tooth-extracted tissues on day 7 in the malnutrition group. One set of mice was used for each day, but an extra mouse for the malnutrition on day 7. un-ext: un-extracted; ext: extracted. Data are presented as mean \pm SD. Statistical significance is indicated by ** $P < 0.01$ and *** $P < 0.001$. One-way ANOVA followed by post hoc Fisher's LSD test was performed.

3.6. ATP concentration after tooth extraction

The ATP concentration in tooth-extracted wound tissues was measured to evaluate the activity of cells in the tissue. After normalization in tooth-un-extracted tissue, the ATP concentration in tooth-extracted wound tissue was more than two times that in tooth-un-extracted tissues in the malnourished group on day 7. This increment was significant compared with that in tooth-extracted wound tissues in the control group (Fig. 6).

4. Discussion

In this study, the delay in wound healing in tooth-extracted socket tissues was validated using a malnourished mouse model. In this tissue, the accumulation of MSCs and bone regeneration were delayed, and prolonged inflammation and relatively large amounts of HMGB1 were detected. Furthermore, an increased M2 $M\phi$ proportion and a relatively large amount of ATP were also detected, suggesting the effects of prolonged inflammatory responses.

MSCs promote healing across a broad range of developmentally unrelated tissues and a myriad of diseases and injury types by accelerating progenitor cell self-renewal, stimulating angiogenesis, and minimizing apoptosis and inflammation [26]. There was little neovascularization or new bone formation in the extraction wound and a decrease in the percentage of MSCs in the immune cells in the malnourished mouse model, which indicates that healing of the extraction wound under malnutrition conditions is delayed. Systemic

inflammation may occur in individuals with anorexia nervosa than in healthy control participants [27]. Nutrition not only supports the function of immune cells, which initiates an effective response against pathogens through the activation of TLRs, but also resolves immune responses rapidly when necessary and avoids any underlying chronic inflammation [28,29]. Many micronutrient deficiencies are responsible for this decline in immunity [30]. The malnutrition-inflammatory score has been widely used to predict chronic kidney disease [31]. However, the ability of dietary intervention to modulate the synthesis of these compounds and their effects on inflammatory processes and metabolic disorders have largely been ignored. Persistent inflammation may be the reason for delayed healing of tooth extraction wounds [32]. In this study, we found that inflammation was slightly reduced 3 days after tooth extraction, but increased on day 7 in malnourished mice, which suggests that inflammation under the state of malnutrition is delayed.

Pattern recognition receptors (PRRs) initiate an immune response by recognizing the structural components of the pathogen to induce the release of molecules from damaged cells as DAMPs. Therefore, DAMPs are considered danger signals that induce inflammatory responses. Moreover, DAMPs mediate the production of pro-inflammatory cytokines to induce non-sterile inflammation by activating TLRs and RAGE receptors [33]. Mild inflammation persists over long periods of time, causing tissue damage and/or fibrosis, leading to irreversible organ dysfunction [13]. HMGB1 is a nucleoprotein that promotes gene transcription by stabilizing nucleosome formation. HMGB1 plays a role in DNA recombination, repair, replication, and gene transcription. It can also be released passively from dying cells or actively secreted

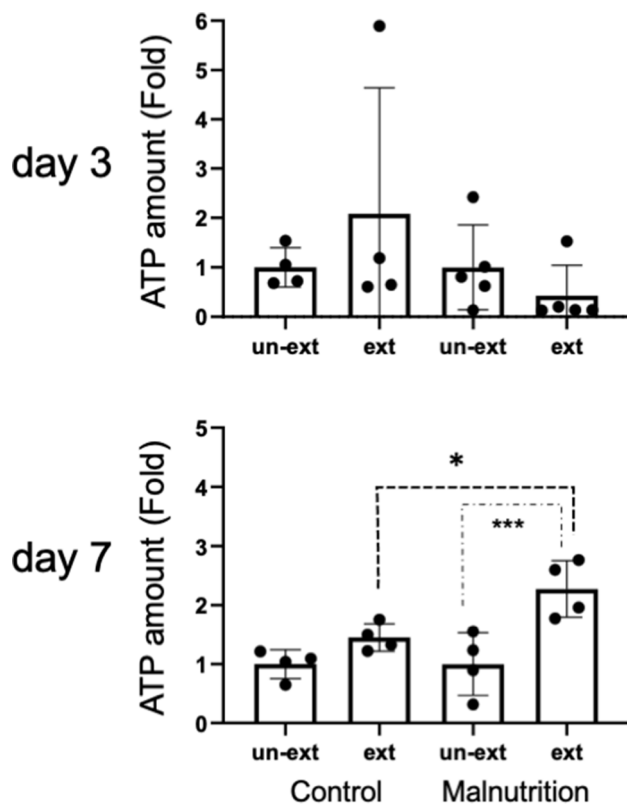


Fig. 6. Increased ATP in gingiva after tooth extraction in malnourished mice. Gingival tissues, including tooth-extracted sockets, were homogenized to determine the ATP concentration. Results were normalized to those of the ATP standard and are presented as fold changes in comparison to the un-extracted group. The ATP concentration varied, but no statistical difference was observed on day 3. However, it increased in the tooth-extracted tissues of malnourished mice on day 7. One set of mice was used for each day, but an extra mouse for the malnutrition on day 3. un-ext: un-extracted; ext: extracted. Data are presented as mean \pm SD. Results were normalized to those of the ATP standard and were presented as fold changes in comparison to the un-extracted group. Statistical significance is indicated by * $P < 0.05$ and *** $P < 0.001$. One-way ANOVA followed by post hoc Fisher's LSD test was performed.

monocytes, macrophages, and myeloid dendritic cells and function as DAMPs [34]. HMGB1 activates multiple receptors (TLR4, TLR2, RAGE, and CXCR4) located in macrophages and mediates the production of TNF- α , IL-1 β , IL-1 α , IL-6, and macrophage inflammatory proteins by promoting nuclear factor (NF)- κ B and mitogen-activated protein kinase [35,36]. The function of HMGB1 largely depends on its location in or outside the nucleus after either active release from cells or passive release upon lytic cell death [37,38]. The secretion of HMGB1 in the gingival tissue increased from the nucleus to the outside 7 days after tooth extraction in a malnourished mouse model. Similarly, the concentration of HMGB1 in the blood increased. In simple terms, the amount of HMGB1 performing the action of DAMPs increased in the gingival tissue and blood of malnourished mice 7 days after tooth extraction.

The interaction of HMGB1 with RAGE receptor is related to the activation of inflammatory response and wound healing in several DAMPs and its accompanying PRR, especially in a non-infectious environment [39]. HMGB1 promotes the secretion of inflammatory factors by activating TLRs or RAGE in macrophages. Macrophages have a key role in the inflammatory phase of tissue repair, and their dynamic plasticity enables the cells to mediate tissue destruction and repair functions. It can be polarized by HMGB1 into classic pro-inflammatory M1 and alternative M2 macrophages [40] and can regulate the transition of different stages of the healing response to promote repair of

damaged tissues [41]. The imbalance of M1/M2 macrophages triggers the development of inflammatory diseases, and macrophage polarization is a target of interest for immunotherapy [35,42,43]. Recent studies have shown that HMGB1 can facilitate the M1 macrophage phenotype in certain inflammatory disease models, mainly based on HMGB1 interaction with TLR receptors [44]. However, HMGB1 can enhance the activity of M2 macrophages in other disease models, especially in a RAGE-dependent manner [35]. Therefore, we explored which receptors are activated by HMGB1 when the healing of tooth extraction wounds is delayed due to persistent inflammation. We found that the proportion of M2 macrophages in total macrophages increased in the malnourished mouse model 7 days after tooth extraction, which suggested that HMGB1 mainly activates RAGE receptors rather than TLR receptors.

IL-1 β is an effective pro-inflammatory cytokine that is associated with wound healing [45,46]. It is produced and secreted by a variety of cell types, including macrophages, which are essential for the host defense response to infection and injury. It is produced as an inactive precursor, termed pro-IL-1 β , in response to the activation of the NF- κ B pathway by DAMPs, which is generally referred to as a priming step. The primed cell must encounter an additional DAMP that activates multiple PRRs to form inflammasomes and induce the processing and secretion of caspase-1-dependent active IL-1 β molecules [47,48]. Among them, HMGB1 is the main DAMP that induces the production of pro-IL-1 β and the maturation of IL-1 β through RAGE [38]. In our study, we found that IL-1 β mRNA gene expression increased in the gingival tissues of malnourished mice 7 days after tooth extraction, which revealed that the increase in extracellular HMGB1 might promote IL-1 β production and lead to prolonged inflammation. CCL2, also known as monocyte chemoattractant protein 1, is a small pro-inflammatory cytokine that is believed to be involved in the early recruitment of macrophages [49]. This increased slightly 3 days after tooth extraction. However, it did not cause inflammatory changes. The wound surface was exposed to oral cavity in this study. There may be alternative reactions if the wound surface was covered by anti-microbial dressing [50], because malnutrition causes alternations in immune reactions.

ATP mainly provides energy to the cells. Changes in nutrients in the environment alter the ATP production pathway [51]. When ATP is rapidly hydrolyzed into ADP or AMP, a large amount of free energy is released to maintain the cell function [52]. On the contrary, ATP is a DAMP that modulates inflammatory cell recruitment [53,54]. ATP acts as an important messenger in cellular processes such as bone formation and absorption, synaptic transmission, blood pressure regulation, and inflammation when it reaches the extracellular milieu due to plasma membrane damage, necrosis, or non-dissolving pathways. ATP regulates HMGB1 release during necrosis [55]. Extracellular ATP stimulates cell migration through the P2X7 receptor and causes the release of HMGB1 through the P2X7 receptor [56,57]. Moreover, ATP significantly enhances the secretion of IL-1 in a time- and dose-dependent manner [58]. Extracellular ATP activates the NLRP3 inflammasome through the P2X7 receptor to induce caspase-1-dependent IL-1 β release, which is one of the most famous and widely used stimuli [56,59]. In this experiment, the extracellular ATP concentration increased in the gingival tissues 7 days after tooth extraction in malnourished mice, demonstrating that the increased extracellular ATP may promote the secretion of HMGB1 from the nucleus and the production of the inflammatory factor IL-1 β .

In summary, 7 days after tooth extraction under the state of malnutrition, ATP is released from the cell to function as a messenger and promotes the increase of HMGB1 secretion by activating the P2X7 receptor. HMGB1 activates the RAGE receptor to promote the polarization of macrophages to M2 macrophages and produce the precursor protein pro-IL-1 β through the NF- κ B pathway. HMGB1 and ATP as DAMPs activate the P2X7 receptor together to generate the assembly of the NLRP3 inflammasome, which triggers the cleavage of the precursor protein pro-IL-1 β by caspase 1 into mature IL-1 β and releases it. These results lead to prolonged inflammation and delayed healing of the extraction wound (Fig. 7).

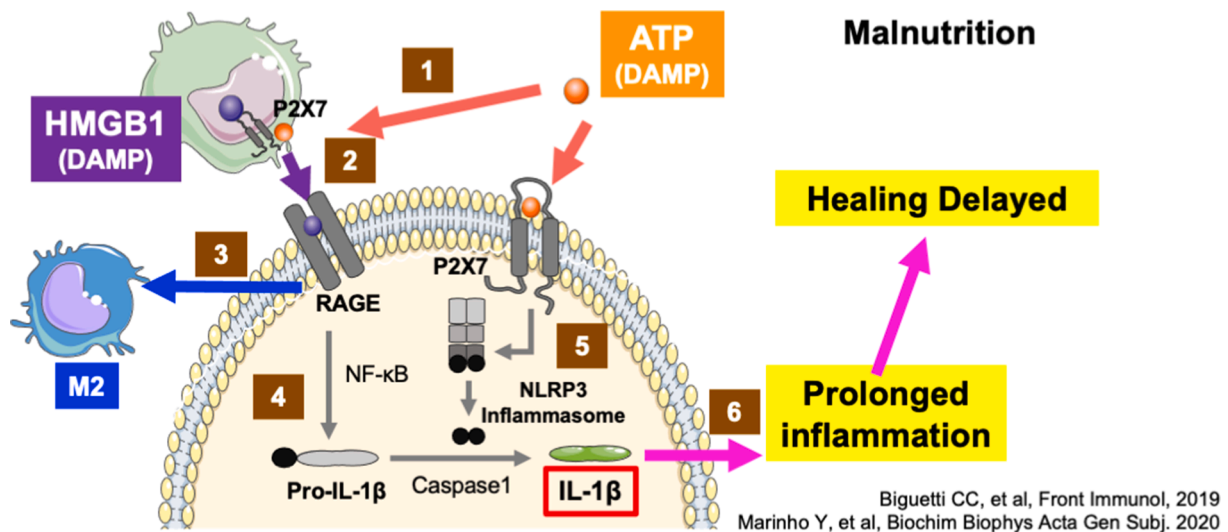


Fig. 7. Schematic representation of the hypothesized mechanism of HMGB1 prolonging inflammation in tooth extraction wounds. (1) Under malnutrition conditions, ATP is secreted from the cell and acts on the P2X7 receptor. (2) The activation of P2X7 receptor promotes the secretion of HMGB1 from macrophages as one of DAMPs. (3) HMGB1 activates the RAGE receptor to promote the polarization of M ϕ to M2 M ϕ . (4) The activated RAGE receptor generates pro-IL-1 β via the NF- κ B pathway. (5) The activation of the P2X7 receptor by HMGB1 and ATP generates the assembly of the NLRP3 inflammasome, triggering the release of mature IL-1 β through caspase 1. (6) IL-1 β prolongs inflammation, leading to delayed healing of tooth extraction wounds.

Unfortunately, significant results of IL-1 β were not obtained in the malnourished mouse model 3 days after tooth extraction. Therefore, the reason for the reduction in inflammation during the initial process of tooth extraction wound healing remains unclear. Similarly, the amount of IL-1 β protein and related receptors such as P2X7, RAGE, and TLRs, and pathways should be evaluated to further improve the understanding of the mechanism of inflammation prolonging malnutrition. It should also be determined whether anti-HMGB1 antibodies promote the healing of tooth extraction wounds in malnourished mice to confirm whether HMGB1 plays a major role in this process. The traditional method of providing nutrition supplements is a long-term treatment process that has little effect on wound healing. Research on the mechanism of delayed wound healing in individuals with malnutrition may provide a new perspective on the targeted promotion or inhibition of short-term diseases associated with malnutrition. Moreover, long-term chronic inflammation related to malnutrition is generally believed to cause a variety of chronic inflammatory diseases, such as chronic kidney disease and neurodegenerative diseases [31,60]. Inhibition of HMGB1 may also help in the treatment of these diseases. Nonetheless, it should be noted that whether anti-HMGB1 antibodies affect prolonged inflammation in malnutrition requires further research.

CRedit authorship contribution statement

Yao Zhang: Methodology, Investigation, Validation, Formal analysis, Writing - original draft, Visualization. **Hidetaka Ideguchi:** Methodology, Investigation, Validation, Resources. **Hiroaki Aoyagi:** Methodology, Investigation, Validation. **Keisuke Yamashiro:** Conceptualization, Methodology, Resources, Writing - review & editing. **Tadashi Yamamoto:** Methodology, Resources, Writing - review & editing. **Masahiro Nishibori:** Resources. **Shogo Takashiba:** Methodology, Resources, Data curation, Writing - review & editing, Supervision.

Declaration of Competing Interest

The authors declare that they have no known competing financial interests or personal relationships that could have appeared to influence the work reported in this paper.

Acknowledgements

The authors would like to thank Dr. Risa Kyoshima-Suzuki for providing advice on experimental techniques, Dr. Anna Hirai for assistance in managing experimental materials, Dr. Zulema Rosalia Arias Martinez for drafting this manuscript.

Data Availability

Main data is included in manuscript. Additional data is available upon reasonable request.

Funding

This study was supported in part by a scholarship from the China Scholarship Council (No. 201708050140; YZ) and JSPS KAKENHI Grant-in-Aid for Scientific Research (JP 19 K10128; KY).

References

- [1] C.A. Corish, L.A. Bardon, Malnutrition in older adults: Screening and determinants, Proc. Nutr. Soc. 78 (2019) 372–379, <https://doi.org/10.1017/S0029665118002628>.
- [2] N.C. Fávoro-Moreira, S. Krausch-Hofmann, C. Matthys, C. Vereecken, E. Vanhauwaert, A. Declercq, G.E. Bekkering, J. Duyck, Risk factors for malnutrition in older adults: A systematic review of the literature based on longitudinal data, Adv. Nutr. 7 (2016) 507–522, <https://doi.org/10.3945/an.115.011254>.
- [3] Z.A. Bhutta, J.A. Berkley, R.H.J. Bandsma, M. Kerac, I. Trehan, A. Briend, Severe childhood malnutrition, Nat. Rev. Dis. Primers. 3 (2017) 17067, <https://doi.org/10.1038/nrdp.2017.67>.
- [4] J.C. Wells, A.L. Sawaya, R. Wibaek, M. Mwangome, M.S. Poullas, C.S. Yajnik, A. Demaio, The double burden of malnutrition: aetiological pathways and consequences for health, Lancet. 395 (2020) 75–88, [https://doi.org/10.1016/S0140-6736\(19\)32472-9](https://doi.org/10.1016/S0140-6736(19)32472-9).
- [5] Y. Alwarawrah, K. Kiernan, N.J. MacIver, Changes in nutritional status impact immune cell metabolism and function, Front. Immunol. 9 (2018) 1055, <https://doi.org/10.3389/fimmu.2018.01055>.
- [6] N. Watson, B. Ding, X. Zhu, R.D. Frisina, Chronic inflammation – inflammaging – in the ageing cochlea: A novel target for future presbycusis therapy, Ageing Res. Rev. 40 (2017) 142–148, <https://doi.org/10.1016/j.arr.2017.10.002>.
- [7] M. Barchitta, A. Maugeri, G. Favara, R.M. San Lio, G. Evola, A. Agodi, G. Basile, Nutrition and wound healing: An overview focusing on the beneficial effects of curcumin, Int. J. Mol. Sci. 20 (2019) 1119, <https://doi.org/10.3390/ijms20051119>.
- [8] H.R.M. de Almeida, E.M.C. Santos, K. Dourado, C. Mota, R. Peixoto, Malnutrition associated with inflammation in the chronic renal patient on hemodialysis, Rev.

- Assoc. Med. Bras. 64 (2018) 837–844, <https://doi.org/10.1590/1806-9282.64.09.837>.
- [9] Y. Zha, Q. Qian, Protein nutrition and malnutrition in CKD and ESRD, *Nutrients*. 9 (2017) 208, <https://doi.org/10.3390/nu9030208>.
- [10] D. Azzolino, P.C. Passarelli, P. De Angelis, G.B. Piccirillo, A. D'addona, M. Cesari, Poor oral health as a determinant of malnutrition and sarcopenia, *Nutrients*. 11 (2019) 2898, <https://doi.org/10.3390/nu1122898>.
- [11] S. Naidoo, N. Myburgh, Nutrition, oral health and the young child, *Matern. Child Nutr.* 3 (2007) 312–321, <https://doi.org/10.1111/j.1740-8709.2007.00115.x>.
- [12] S.W. City, L.J. Cowan, Z. Wingfield, J. Stechmiller, Optimizing nutrition care for pressure injuries in hospitalized patients, *Adv. Wound Care*. 8 (2019) 309–322, <https://doi.org/10.1089/wound.2018.0925>.
- [13] Z. Radak, F. Torma, I. Berkes, S. Goto, T. Mimura, A. Posa, L. Balogh, I. Boldogh, K. Suzuki, M. Higuchi, E. Koltai, Exercise effects on physiological function during aging, *Free Radic. Biol. Med.* 132 (2019) 33–41, <https://doi.org/10.1016/j.freeradbiomed.2018.10.444>.
- [14] M.M. Fouda, A.M. Abdel-Mohsen, H. Ebaid, I. Hassan, J. Al-Tamimi, R.M. Abdel-Rahman, A. Metwalli, I. Alhazza, A. Rady, A. El-Faham, J. Jancar, Wound healing of different Molecular weight of hyaluronan; In vivo study, *Int J Biol Macromol.* 89 (2016) 582–591, <https://doi.org/10.1016/j.ijbiomac.2016.05.021>.
- [15] M.R. El-Aassar, O.M. Ibrahim, M. Fouda, N.G. El-Beheri, M.M. Agwa, Wound healing of nanofiber comprising Polygalacturonic/Hyaluronic acid embedded silver nanoparticles: In-vitro and in-vivo studies, *Carbohydr Polym.* 238 (2020), 116175, <https://doi.org/10.1016/j.carbpol.2020.116175>.
- [16] S. Homaeigohar, A.R. Boccaccini, Antibacterial biohybrid nanofibers for wound dressings, *Acta Biomater.* 107 (2020) 25–49, <https://doi.org/10.1016/j.actbio.2020.02.022>.
- [17] C.V. Laur, T. McNicholl, R. Valaitis, H.H. Keller, Malnutrition or frailty? Overlap and evidence gaps in the diagnosis and treatment of frailty and malnutrition, *Appl. Physiol. Nutr. Metab.* 42 (2017) 449–458, <https://doi.org/10.1139/apnm-2016-0652>.
- [18] S.C. Qi, C. Cui, Y.H. Yan, G.H. Sun, S.R. Zhu, Effects of high-mobility group box 1 on the proliferation and odontoblastic differentiation of human dental pulp cells, *Int. Endod. J.* 46 (2013) 1153–1163, <https://doi.org/10.1111/iej.12112>.
- [19] H. Yang, H. Wang, U. Andersson, Targeting inflammation driven by HMGB1, *Front. Immunol.* 11 (2020) 484, <https://doi.org/10.3389/fimmu.2020.00484>.
- [20] H. Aoyagi, K. Yamashiro, C. Hirata-Yoshihara, H. Ideguchi, M. Yamasaki, M. Kawamura, T. Yamamoto, S. Kochi, H. Wake, M. Nishibori, S. Takashiba, HMGB1-induced inflammatory response promotes bone healing in murine tooth extraction socket, *J. Cell. Biochem.* 119 (2018) 5481–5490, <https://doi.org/10.1002/jcb.26710>.
- [21] C. Yoshihara-Hirata, K. Yamashiro, T. Yamamoto, H. Aoyagi, H. Ideguchi, M. Kawamura, R. Suzuki, M. Ono, H. Wake, M. Nishibori, S. Takashiba, Anti-HMGB1 neutralizing antibody attenuates periodontal inflammation and bone resorption in a murine periodontitis model, *Infect. Immun.* 86 (2018) e00111–18, <https://doi.org/10.1128/IAI.00111-18>.
- [22] G.M. Anstead, B. Chandrasekar, W. Zhao, J. Yang, L.E. Perez, P.C. Melby, Malnutrition alters the innate immune response and increases early visceralization following *Leishmania donovani* infection, *Infect. Immun.* 69 (2001) 4709–4718, <https://doi.org/10.1128/IAI.69.8.4709-4718.2001>.
- [23] K.J. Livak, T.D. Schmittgen, Analysis of relative gene expression data using real-time quantitative PCR and the 2- $\Delta\Delta$ CT method, *Methods*. 25 (2001) 402–408, <https://doi.org/10.1006/meth.2001.1262>.
- [24] L. de Almeida, A. Dorfleutner, C. Stehlik, In vivo analysis of neutrophil infiltration during LPS-induced peritonitis, *Bio. Protoc.* 6 (2016), e1945, <https://doi.org/10.21769/BioProtoc.1945>.
- [25] K. Phan, Y. He, R. Pickford, S. Bhatia, J.S. Katzeff, J.R. Hodges, O. Piguet, G. M. Halliday, W.S. Kim, Uncovering pathophysiological changes in frontotemporal dementia using serum lipids, *Sci. Rep.* 10 (2020) 3640, <https://doi.org/10.1038/s41598-020-60457-w>.
- [26] J.L. Spees, R.H. Lee, C.A. Gregory, Mechanisms of mesenchymal stem/stromal cell function, *Stem Cell Res. Ther.* 7 (2016) 125, <https://doi.org/10.1186/s13287-016-0363-7>.
- [27] B. Dalton, I.C. Campbell, R. Chung, G. Breen, U. Schmidt, H. Himmerich, Inflammatory markers in anorexia nervosa: An exploratory study, *Nutrients*. 10 (2018) 1573, <https://doi.org/10.3390/nu10111573>.
- [28] C.E. Childs, P.C. Calder, E.A. Miles, Diet and immune function, *Nutrients*. 11 (2019) 1933, <https://doi.org/10.3390/nu11081933>.
- [29] K. Suzuki, Chronic inflammation as an immunological abnormality and effectiveness of exercise, *Biomolecules*. 9 (2019) 223, <https://doi.org/10.3390/biom9060223>.
- [30] S. Maggini, A. Pierre, P.C. Calder, Immune function and micronutrient requirements change over the life course, *Nutrients*. 10 (2018) 1531, <https://doi.org/10.3390/nu10101531>.
- [31] D. Jagadeswaran, E. Indhumathi, A.J. Hemamalini, V. Sivakumar, P. Soundararajan, M. Jayakumar, Inflammation and nutritional status assessment by malnutrition inflammation score and its outcome in pre-dialysis chronic kidney disease patients, *Clin. Nutr.* 38 (2019) 341–347, <https://doi.org/10.1016/j.clnu.2018.01.001>.
- [32] R. Zhao, H. Liang, E. Clarke, C. Jackson, M. Xue, Inflammation in chronic wounds, *Int. J. Mol. Sci.* 17 (2016) 2085, <https://doi.org/10.3390/ijms17122085>.
- [33] O. Takeuchi, S. Akira, Pattern recognition receptors and inflammation, *Cell*. 140 (2010) 805–820, <https://doi.org/10.1016/j.cell.2010.01.022>.
- [34] M. Son, A. Porat, M. He, J. Suurmond, F. Santiago-Schwarz, U. Andersson, T. R. Coleman, B.T. Volpe, K.J. Tracey, Y. Al-Abed, B. Diamond, C1q and HMGB1 reciprocally regulate human macrophage polarization, *Blood*. 128 (2016) 2218–2228, <https://doi.org/10.1182/blood-2016-05-719757>.
- [35] C.C. Bigueti, F. Cavalla, E.V. Silveira, A.P. Tabanez, C.F. Francisconi, R. Taga, A.P. Campanelli, A.P.F. Trombone, D.C. Rodrigues, G.P. Garlet, HMGB1 and RAGE as essential components of Ti osseointegration process in mice, *Front. Immunol.* 10 (2019) 709, <https://doi.org/10.3389/fimmu.2019.00709>.
- [36] M. Lommatsch, P. Stoll, Novel strategies for the treatment of asthma, *Allergo J. Int.* 25 (2016) 11–17, <https://doi.org/10.1007/s40629-016-0093-5>.
- [37] C. Mendonça Gorgulho, P. Murthy, L. Liotta, V. Espina, M.T. Lotze, Different measures of HMGB1 location in cancer immunology, *Methods Enzymol.* 629 (2019) 195–217, <https://doi.org/10.1016/bs.mie.2019.10.011>.
- [38] M. Deng, M.J. Scott, J. Fan, T.R. Billiar, Location is the key to function: HMGB1 in sepsis and trauma-induced inflammation, *J. Leukoc. Biol.* 106 (2019) 161–169, <https://doi.org/10.1002/JLB.3MIR1218-497R>.
- [39] S. Tanchareon, S. Gando, S. Binita, T. Nagasato, K. Kikuchi, Y. Nawa, P. Dararat, M. Yamamoto, S. Narkpinit, I. Maruyama, HMGB1 promotes intraoral palatal wound healing through RAGE-dependent mechanisms, *Int. J. Mol. Sci.* 17 (2016) 1961, <https://doi.org/10.3390/ijms17111961>.
- [40] S. Colin, G. Chinetti-Gbaguidi, B. Staels, Macrophage phenotypes in atherosclerosis, *Immunol. Rev.* 262 (2014) 153–166, <https://doi.org/10.1111/imr.12218>.
- [41] J.C. Gensel, B. Zhang, Macrophage activation and its role in repair and pathology after spinal cord injury, *Brain Res.* 1619 (2015) 1–11, <https://doi.org/10.1016/j.brainres.2014.12.045>.
- [42] S.C. Funes, M. Rios, J. Escobar-Vera, A.M. Kalergis, Implications of macrophage polarization in autoimmunity, *Immunology*. 154 (2018) 186–195, <https://doi.org/10.1111/imm.12910>.
- [43] A.E. Boniakowski, A.S. Kimball, B.N. Jacobs, S.L. Kunkel, K.A. Gallagher, Macrophage-mediated inflammation in normal and diabetic wound healing, *J. Immunol.* 199 (2017) 17–24, <https://doi.org/10.4049/jimmunol.1700223>.
- [44] Z. Su, P. Zhang, Y. Yu, H. Lu, Y. Liu, P. Ni, X. Su, D. Wang, Y. Liu, J. Wang, H. Shen, W. Xu, H. Xu, HMGB1 facilitated macrophage reprogramming towards a proinflammatory M1-like phenotype in experimental autoimmune myocarditis development, *Sci. Rep.* 6 (2016) 21884, <https://doi.org/10.1038/srep21884>.
- [45] Y.S. Yi, Regulatory roles of flavonoids on inflammasome activation during inflammatory responses, *Mol. Nutr. Food Res.* 62 (2018) 1800147, <https://doi.org/10.1002/mnfr.201800147>.
- [46] Y. Li, Y. Wang, L. Zhou, M. Liu, G. Liang, R. Yan, Y. Jiang, J. Hao, X. Zhang, X. Hu, Y. Huang, R. Wang, Z. Yin, J. Wu, G. Luo, W. He, V γ 4 T cells inhibit the pro-healing functions of dendritic epidermal T cells to delay skin wound closure through IL-17A, *Front. Immunol.* 9 (2018) 240, <https://doi.org/10.3389/fimmu.2018.00240>.
- [47] G. Lopez-Castejon, D. Brough, Understanding the mechanism of IL-1 β secretion, *Cytokine Growth Factor Rev.* 22 (2011) 189–195, <https://doi.org/10.1016/j.cytogfr.2011.10.001>.
- [48] S.H. Pulugulla, T.A. Packard, N.L.K. Galloway, Z.W. Grimmett, G. Doitsh, J. Adamik, D.L. Galson, W.C. Greene, P.E. Auron, Distinct mechanisms regulate IL1B gene transcription in lymphoid CD4 T cells and monocytes, *Cytokine*. 111 (2018) 373–381, <https://doi.org/10.1016/j.cyto.2018.10.001>.
- [49] X. Sun, D.J. Glynn, L.J. Hodson, C. Huo, K. Britt, E.W. Thompson, L. Woolford, A. Evdokiou, J.W. Pollard, S.A. Robertson, W.V. Ingman, CCL2-driven inflammation increases mammary gland stromal density and cancer susceptibility in a transgenic mouse model, *Breast Cancer Res.* 19 (2017) 4, <https://doi.org/10.1186/s13058-016-0796-z>.
- [50] M.R. El-Aassar, O.M. Ibrahim, M.M.G. Fouda, H. Fakhry, J. Ajarem, S.N. Maooda, A.A. Allam, E.E. Hafez, Wound dressing of chitosan-based-crosslinked gelatin/polyvinyl pyrrolidone embedded silver nanoparticles, for targeting multidrug resistance microbes, *Carbohydr. Polym.* 255 (2021), 117484, <https://doi.org/10.1016/j.carbpol.2020.117484>.
- [51] H. Imamura, K.P. Huynh Nhat, H. Togawa, K. Saito, R. Iino, Y. Kato-Yamada, T. Nagai, H. Noji, Visualization of ATP levels inside single living cells with fluorescence resonance energy transfer-based genetically encoded indicators, *Proc. Natl. Acad. Sci. U. S. A.* 106 (2009) 15651–15656, <https://doi.org/10.1073/pnas.0904764106>.
- [52] B. Drew, C. Leeuwenburgh, Method for measuring ATP production in isolated mitochondria: ATP production in brain and liver mitochondria of Fischer-344 rats with age and caloric restriction, *Am. J. Physiol. Regul. Integr. Comp. Physiol.* 285 (2003) 1259–1267, <https://doi.org/10.1152/ajpregu.00264.2003>.
- [53] M. Dosch, J. Gerber, F. Jebbawi, G. Beldi, Mechanisms of ATP release by inflammatory cells, *Int. J. Mol. Sci.* 19 (2018) 1222, <https://doi.org/10.3390/ijms19041222>.
- [54] A. Inami, H. Kiyono, Y. Kurashima, ATP as a pathophysiologic mediator of bacteria-host crosstalk in the gastrointestinal tract, *Int. J. Mol. Sci.* 19 (2018) 2371, <https://doi.org/10.3390/ijms19082371>.
- [55] R. Kang, Q. Zhang, H.J. Zeh, M.T. Lotze, D. Tang, HMGB1 in cancer: Good, bad, or both? *Clin. Cancer Res.* 19 (2013) 4046–4057, <https://doi.org/10.1158/1078-0432.CCR-13-0495>.
- [56] Y. Marinho, C. Marques-da-Silva, P.T. Santana, M.M. Chaves, A.S. Tamura, T. P. Rangel, I.V. Gomes-e-Silva, M.Z.P. Guimarães, R. Coutinho-Silva, MSU Crystals induce sterile IL-1 β secretion via P2X7 receptor activation and HMGB1 release, *Biochim. Biophys. Acta Gen. Subj.* 1864 (2020), 129461, <https://doi.org/10.1016/j.bbagen.2019.129461>.
- [57] S. Hiramoto, M. Tsubota, K. Yamaguchi, K. Okazaki, A. Sakaegi, Y. Toriyama, J. Tanaka, F. Sekiguchi, H. Ishikura, H. Wake, M. Nishibori, H. Du Nguyen, T. Okada, N. Toyooka, A. Kawabata, Cystitis-related bladder pain involves ATP-dependent HMGB1 release from macrophages and its downstream H2S/Cav3.2 signaling in mice, *Cells*. 9 (2020) 1748, <https://doi.org/10.3390/cells9081748>.

- [58] H. Ren, Y. Teng, B. Tan, X. Zhang, W. Jiang, M. Liu, W. Jiang, B. Du, M. Qian, Toll-like receptor-triggered calcium mobilization protects mice against bacterial infection through extracellular ATP release, *Infect. Immun.* 82 (2014) 5076–5085, <https://doi.org/10.1128/IAI.02546-14>.
- [59] E.K. Jo, J.K. Kim, D.M. Shin, C. Sasakawa, Molecular mechanisms regulating NLRP3 inflammasome activation, *Cell. Mol. Immunol.* 13 (2016) 148–159, <https://doi.org/10.1038/cmi.2015.95>.
- [60] D. Wlodarek, Role of ketogenic diets in neurodegenerative diseases (Alzheimer's disease and Parkinson's disease), *Nutrients.* 11 (2019) 169, <https://doi.org/10.3390/nu11010169>.